Diagnostics of air plasma ablated by 1064 nm laser pulses

Wenfeng Luo (罗文峰)*, Wei Zhao (赵 卫), Yixiang Duan (段忆翔), and Haojing Wang (王浩静)

State Key Laboratory of Transient Optics and Photonics, Xi'an Institute of Optics and Precision Mechanics, Chinese Academy of Sciences, Xi'an 710119, China

**Corresponding author: luowf@opt.ac.cn*

Received December 15, 2010; accepted January 6, 2011; posted online June 27, 2011

The characteristics of air plasma are studied using laser-induced breakdown spectroscopy at room temperature in air at atmospheric pressure. The electron temperature of 20796 K is determined using the Boltzmann plot method with six ionic nitrogen lines at 444.703, 463.054, 500.515, 566.663, 594.165, and 648.205 nm. The electron number density inferred by measuring the Stark broadened profile of well-isolated H_α line (656.273 nm) is 1.83×10^{17} cm^{-3}. The hypotheses of the local thermodynamic equilibrium and optically thin plasma are verified based on the experimental results. These results are beneficial for better understanding of the terahertz (THz) wave generation in pulsed laser induced air plasma.

OCIS codes: 020.0020, 140.0140, 300.0300.

doi: 10.3788/COL201109.S10303.

Laser-induced air plasmas (LIAP) have acquired great interest from researchers in recent years as spectroscopic sources. In this method, a short-pulse laser is focused into air, and localized plasma is produced when the breakdown threshold is met. The collection and spectral analysis of the plasma emissions allow qualitative and quantitative analysis of atomic species[1−4]. Due to its simplicity, rapidity, non-contact and *in situ* analysis, and high temporal and spatial resolution, laser-induced breakdown spectroscopy (LIBS) has been applied in many fields, such as elemental analysis, environmental monitoring, toxic substance detection, thin film deposition, laser-guided lightning, and laser ignition[5−7].

Aside from these applications, terahertz (THz) wave generation in LIAP has also attracted considerable attention recently, and experiments showed that ambient air with a composition of about 78% nitrogen exhibited remarkable performance for the generation and detection of THz waves with femtosecond laser pulses[8−10]. Das *et al.* reported tunable narrowband THz waveforms from 2.5 to 7.5 THz, which were generated from LIAP using shaped optical pulse[8]. In 2006, Dai *et al.* reported the first demonstration of the coherent detection of broadband THz waves with ambient air by introducing the second-harmonic component of white light in LIAP as a local oscillator dependent on plasma density[9]. Their results also showed that the detection of THz waves in air could be categorized as incoherent, hybrid, and coherent detections depending on the air ionization process, which is related to the plasma parameters[3,4,9,11]. Therefore, the precise knowledge of the electron density and electron temperature is a necessary requirement for understanding such kinds of processes.

To advance this understanding further, the characteristics of LIAP using a 1064-nm Nd:YAG laser were investigated spectroscopically. The plasma temperature was inferred using the Boltzmann plot method with several N(II) lines, whereas the electron number density was determined by measuring the Stark broadened line profile of H_α line. At the same time, local thermodynamic equilibrium (LTE) and self-absorption of plasma were examined based on the experimental results.

The experimental setup used for LIAP is shown in Fig. 1. Laser pulses from a Q-switched Nd:YAG laser (1064 nm, 19.7-ns full-width at half-maximan (FWHM), 1 Hz, 434 ± 73 mJ/pulse, SGR, Beamtech Optronics) were focused into air using a quartz lens (f = 150 mm). The intensity of the laser light within the focal volume was estimated to be 6.8×10^{12} W/cm^2[12]. One end (200 μm in diameter) of a fiber bundle was used to collect the light emitted from the air plasma, and its other five ends were connected to the entrance slits (10 μm in diameter) of the broadband spectrometer (200−720 nm range, 0.06−0.08 optical resolution with 2400−1800 grooves/mm, AvanSpec-2048FT-5 Avantes, Holland), which was triggered by the Q-switch of the Nd:YAG laser. The output data were averaged for 10 laser shots and stored in a personal computer through AvaSoft-LIBS software for subsequent analysis. All the experiments were performed at room temperature in air at atmospheric pressure.

Figure 2 shows the typical emission spectra of LIAP with irradiance of 6.8×10^{12} W/cm^2. The plasma spectrum consisted of an intense continuum emission and a number of ionic lines of element nitrogen (N) and oxygen (O). At the same time, the strong H_α at 656.273 nm was observed, which should originate from the very small concentration of water in the ambient air because of the natural humidity present. At the initial stage of the plasma process, the signal was mostly dominated by the continuum emission. Lin *et al.* demonstrated that the stronger short wavelength continuous spectrum is caused by bremsstrahlung radiation of electrons in the plasma, and the weaker long wavelength continuous

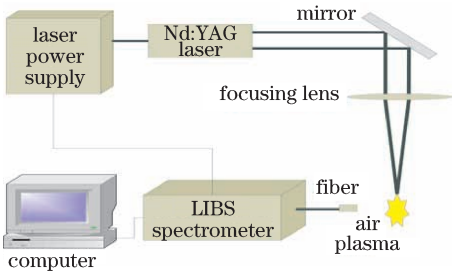

Fig. 1. Experimental setup.

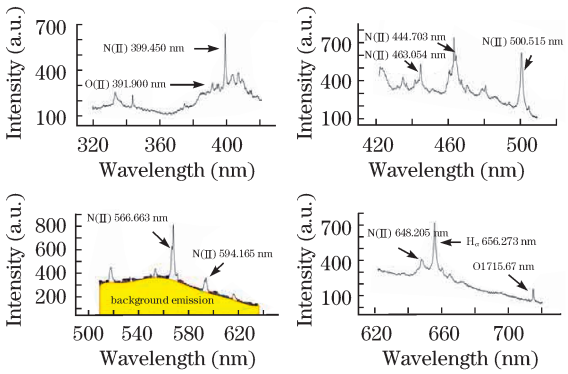

Fig. 2. Spectra of LIAP.

spectrum is caused by electron and ion recombination[13]. As time progresses, continuum background emission diminishes, whereas the ionic and atomic emission lines become dominant[3,4]. To obtain a good compromise between the signal background ratio and the emission lines, the delay time (defined as the interval between the laser shot and the initiation of data acquisition) and the integrated time were set to 7 μs and 2 ms, respectively, in our experiments. The assignments of these atomic and ionic lines indicated by the arrows were performed using the NIST database[14].

In Fig. 2, the background emission of LIAP was strong and complex. To calculate and subtract the continuum emission more precisely, a sixth-degree polynomial function

$$Y = 2.83624 \times 10^7 - 278105.85799X + 1129.79816X^2 - 2.43297X^3 + 0.00293X^4 - 1.86524 \times 10^{-6}X^5 + 4.91158 \times 10^{-10}X^6 \quad (1)$$

is used to fit the background. An illustration with the coefficient of regression of 0.99 is also presented in Fig. 2.

As the properties of LIAP are characterized by the plasma temperature T_e, the electron density N_e, and the number density of the emitting species, their measurements are important to understand the occurring plasma processes, i.e., vaporization, dissociation, excitation, and ionization. The emitted spectral line intensity is a measure of the population of the corresponding energy level of a certain species in the plasma. Under the assumptions of LTE and optically thin plasma[3,4], T_e can be obtained from the information on the spectral line intensity because the population distribution is a function of T_e according to Boltzmann equation. The linearization of Boltzmann plot equation is[1]

$$\ln\left(\frac{\lambda_{mn} I_{mn}}{h c g_m A_{mn}}\right) = -\frac{E_m}{kT_e} + \ln\left[\frac{N(T)}{U(T)}\right], \quad (2)$$

where λ_{mn} is the wavelength, A_{mn} is the transition probability, g_m is the statistical weight of the upper level, h is the Plank constant, c is the speed of light in vacuum, E_m is the upper level energy, T_e is the electron temperature, k is the Boltzmann constant, $N(T)$ is the total number density of species, and $U(T)$ is the partition function. A plot of the left-hand side of Eq. (2) versus E_m has a slope of $-1/kT_e$, and the plasma temperature can be obtained through linear regression even without $N(T)$ or $U(T)$.

The intensities of a series of ionic nitrogen lines (i.e., 444.703, 463.054, 500.515, 566.663, 594.165, and 648.205 nm) were measured; their corresponding parameters can be found in the NIST database[14]. A typical Boltzmann plot for temperature determination is shown in Fig. 3. The plasma temperature of 20796 K was calculated from the slope of -6.9×10^{-5}.

The determination of electron number density is important for understanding the fundamental characteristics of plasma sources because electrons play an essential role in energy transfer and many other processes within analytical plasmas[3]. One of the most common methods for calculating N_e in analytical plasmas is to measure the Stark broadening of the emission lines of the plasma gas. In laser-induced plasma, the dominant broadening mechanism of the line profile is Stark broadening, which results from the collisions with charged species. Note that other broadening mechanisms, including the Doppler and the natural ones, are generally negligible[15].

To better characterize the LIAP, the electron density was calculated based on the Stark broadening of the H_α line (656.273 nm) produced in the presence of a very small concentration of water in the ambient atmosphere. Historically, the H_α line was successfully used to diagnose several kinds of plasma (e.g., solar flares, activity of the sun, etc.) because of its attractive features. This line is not only a well-isolated strong line but is also free from self-absorption. Moreover, its Stark width is relatively large and symmetric, which is related to the electron density through[16]

$$N_e = 8.02 \times 10^{12} (\Delta\lambda_{1/2}/\alpha_{1/2})^{3/2}, \quad (3)$$

where $\Delta\lambda_{1/2}$ is the FWHM of the H_α line, and $\alpha_{1/2}$ is the half width of the reduced Stark profile[17].

A typical Stark broadened line profile is approximately Lorentzian. The profile of the measured H_α line shown in Fig. 4 fits well with a typical Lorentzian function. The electron density of 1.83×10^{17} cm^{-3} was inferred from the experimental results, which was consistent with the value obtained by other authors[16].

To use N(II) lines to infer the electron temperature and to use H_α line to calculate the electron density, LTE needs to be fulfilled. This requires the collisional excitation and de-excitation processes to dominate the radiative processes as well as a minimum electron density[1,3,4]. The lower limit of the electron density where the plasma will be in LTE is calculated through[18]

$$N_e \geq 1.4 \times 10^{14} T^{1/2} (\Delta E)^3, \quad (4)$$

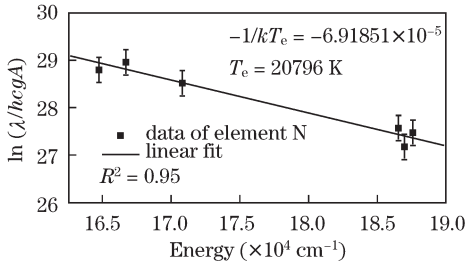

Fig. 3. Boltzmann plot of N(II) lines.

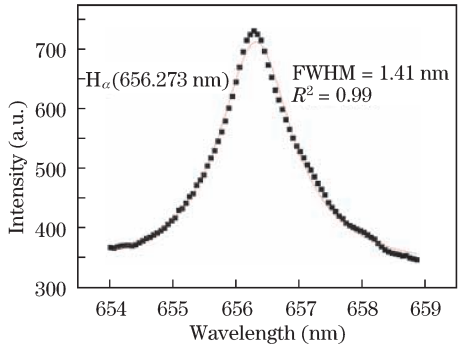

Fig. 4. Lorentzian profile of H_α.

where ΔE is the energy difference between the states, and T is the temperature of the plasma. In the present case, the largest energy transition was 2.79 eV for N(II) at 444.703 nm; the electron density lower limit value was 4.08×10^{15} cm^{-3} less than the experimentally calculated density 1.83×10^{17} cm^{-3}, verifying that the LIAP was in LTE.

Moreover, the absence of a dip at the center as well as the line symmetry of the H_α line shown in Fig. 4 further confirmed the plasma to be optically thin[16].

LIBS is applied to the analysis of air plasma. Air plasma is produced by focusing a 434-mJ pulsed Nd:YAG laser into the air at atmospheric pressure. The parameters of air plasma are studied in detail in terms of their spectra, electron density, and electron temperature. The value of N_e is 1.83×10^{17} cm^{-3}, which is inferred from the Lorentzian fitting of H_α line at 656.273 nm, whereas the value of T_e is 20796 K using the Boltzmann plot method with a set of N(II) lines at 444.703, 463.054, 500.515, 566.663, 594.165, and 648.205 nm. Experiments confirm that the LIAP is in LTE and is free from self-absorption or self-reversal. These results should be beneficial in the better understanding of the THz wave generation in pulsed LIAP.

This work was supported by the Chinese Academy of Sciences/State Administration of Foreign Experts Affairs. International Partnership Program for Creative Research Teams.

References

1. C. Aragón and J. A. Aguilera, Spectrochim. Acta Part B **63,** 893 (2008).
2. L. Wang, C. J. Zhang, and Y. Feng, Chin. Opt. Lett. **6,** 5 (2008).
3. D. A. Cremers and L. J. Radziemski, *Handbook of Laser-Induced Breakdown Spectroscopy* (John Wiley and Sons, Chichester, 2006).
4. J. P. Singh, and S. N. Thakur, *Laser-Induced Breakdown Spectroscopy* (Elsevier Science BV, Amsterdam, 2007).
5. J. J. Camacho, M. Santos, L. Diaz, L. J. Juan, and J. M. L. Poyato, Appl. Phys. A **99,** 159 (2010).
6. N. Kawahara, J. L. Beduneau, T. Nakayama, E. Tomita, and Y. Ikeda, Appl. Phys. B **86,** 605 (2007).
7. Z. X. Lin, J. Q. Wu, F. L. Sun, and S. S. Gong, Appl. Opt. **49,** C80 (2010).
8. J. Das, and M. Yamaguchi, Opt. Express **18,** 7038 (2010).
9. J. M. Dai, X. Xie, and X. C. Zhang, Phys. Rev. Lett. **97,** 103903 (2006).
10. X. Xie, J. M. Dai, and X. C. Zhang, Phys. Rev. Lett. **96,** 075005 (2006).
11. M. Sabsabi and P. Cielo, Appl. Spectrosc. **49,** 499 (1995).
12. R. E. Russo, X. L. Mao, H. Liu, J. Gonzalez, and S. S. Mao, Talanta **57,** 425 (2002).
13. Z. X. Lin, J. Q. Wu, F. L. Sun, and S. S. Gong, Appl. Opt. **49,** C80 (2010).
14. Ralchenko, Yu., Kramida, A. E., Reader, J., and NIDT ASD Team (2010), "NIST Atomic Spectra Database (cersion 4.0)", http://physics.nist.gov/PhysRefData/ASD/index.html.
15. H. C. Liu, X. L. Mao, J. H. Yoo, and R. E. Russo, Spectrochim. Spectrochim. Acta B **54,** 1607 (1999).
16. A. M. El Sherbini, H. Hegazy, and Th. M. El Sherbini, Spectrochim. Acta B **61,** 532 (2006).
17. P. Kepple and H. R. Griem, Phys. Rev. **173,** 317 (1968).
18. G. Abdellatif and H. Imam, Spectrochim. Acta B **57,** 1155 (2002).